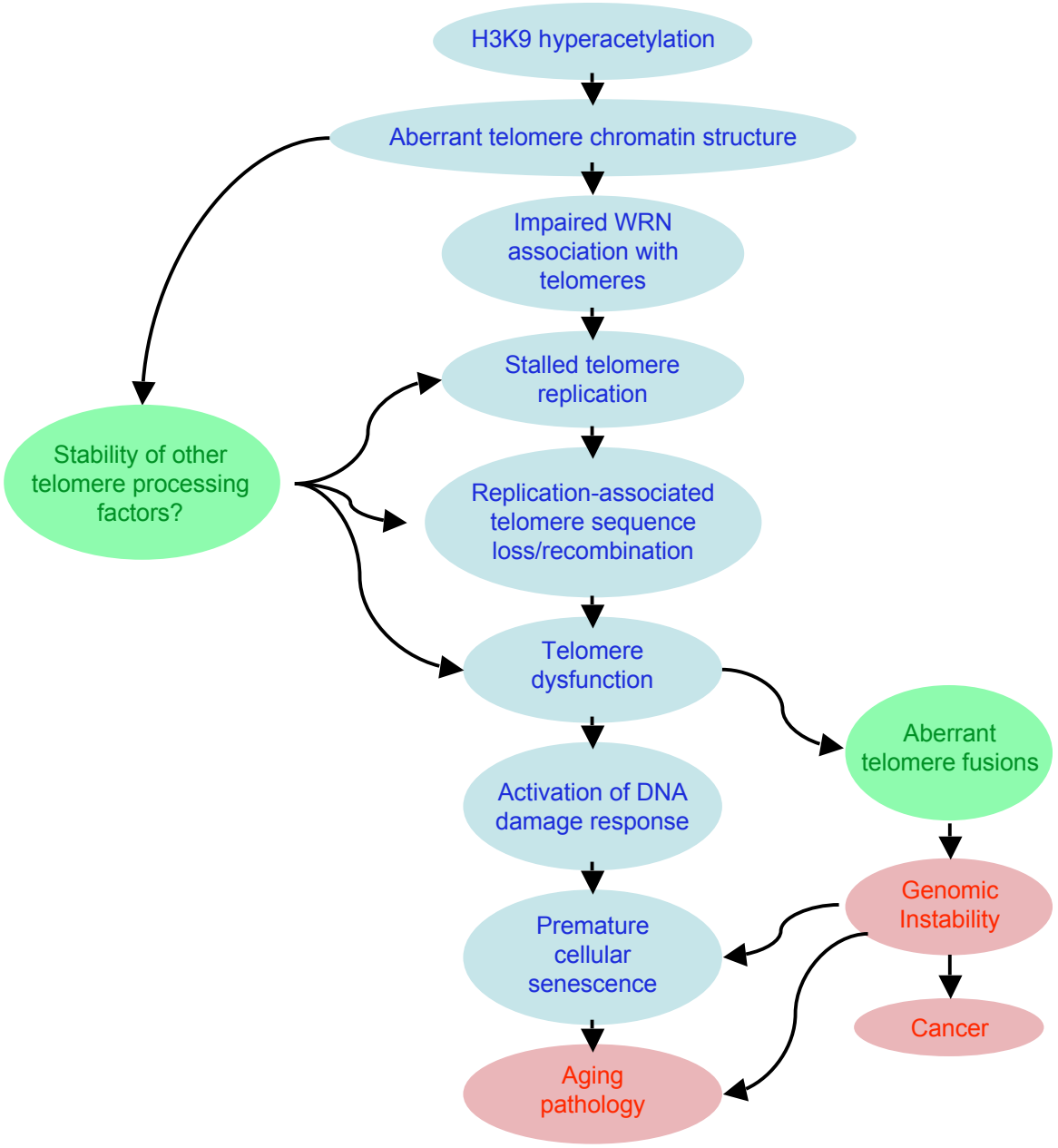

Supplemental Figure 1. Model. We propose the following order of events when SIRT6 is inactivated in human cells. Loss of SIRT6 deacetylase activity results in H3K9 hyperacetylation and an abnormal telomeric chromatin state. The altered telomeric chromatin structure then contributes to impaired S-phase association of WRN with telomeres. The resulting insufficient telomeric WRN leads to stalled telomere replication, stochastic telomere sequence loss and recombination, and delayed S-phase completion. As a result of the stochastic telomere sequence loss, telomere dysfunction leads to genomic instability with chromosomal fusions, and premature cellular senescence.

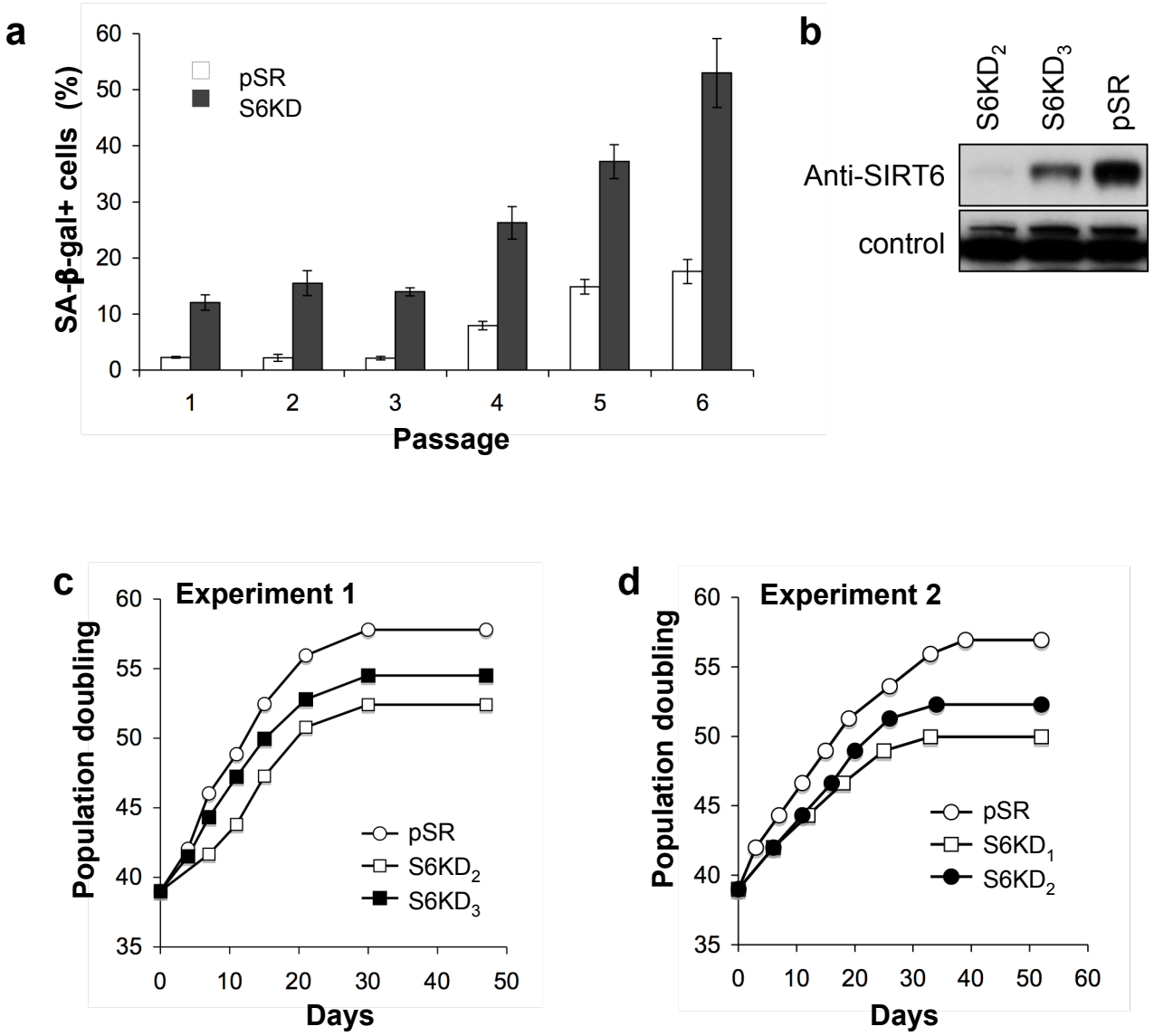

Supplemental Figure 2. Premature replicative senescence of SIRT6 knock-down cells. **a,** Senescence-associated β-galactosidase (SA-β-gal) staining of S6KD and control pSR cultures over the course of a serial passaging experiment. Knock-down was generated at population doubling (PD) 30, and passage 1 corresponds to PD33, when SA-β-gal staining begins to be apparent. **b**, Western analysis of SIRT6 expression in WI-38 cells expressing multiple independent SIRT6 shRNAs by retroviral transduction, compared to pSR control cells. **c, d,** Serial passaging experiments showing cumulative population doublings of cell cultures on the indicated days following induction of SIRT6 knock-down. Western analysis of $S6KD_1$ is shown in Fig.1. Note that the effect of $S6KD_2$ and $S6KD_3$ on replicative lifespan are less dramatic than that of $S6KD_1$, consistent with the relative efficiency of the knock-down shRNAs.

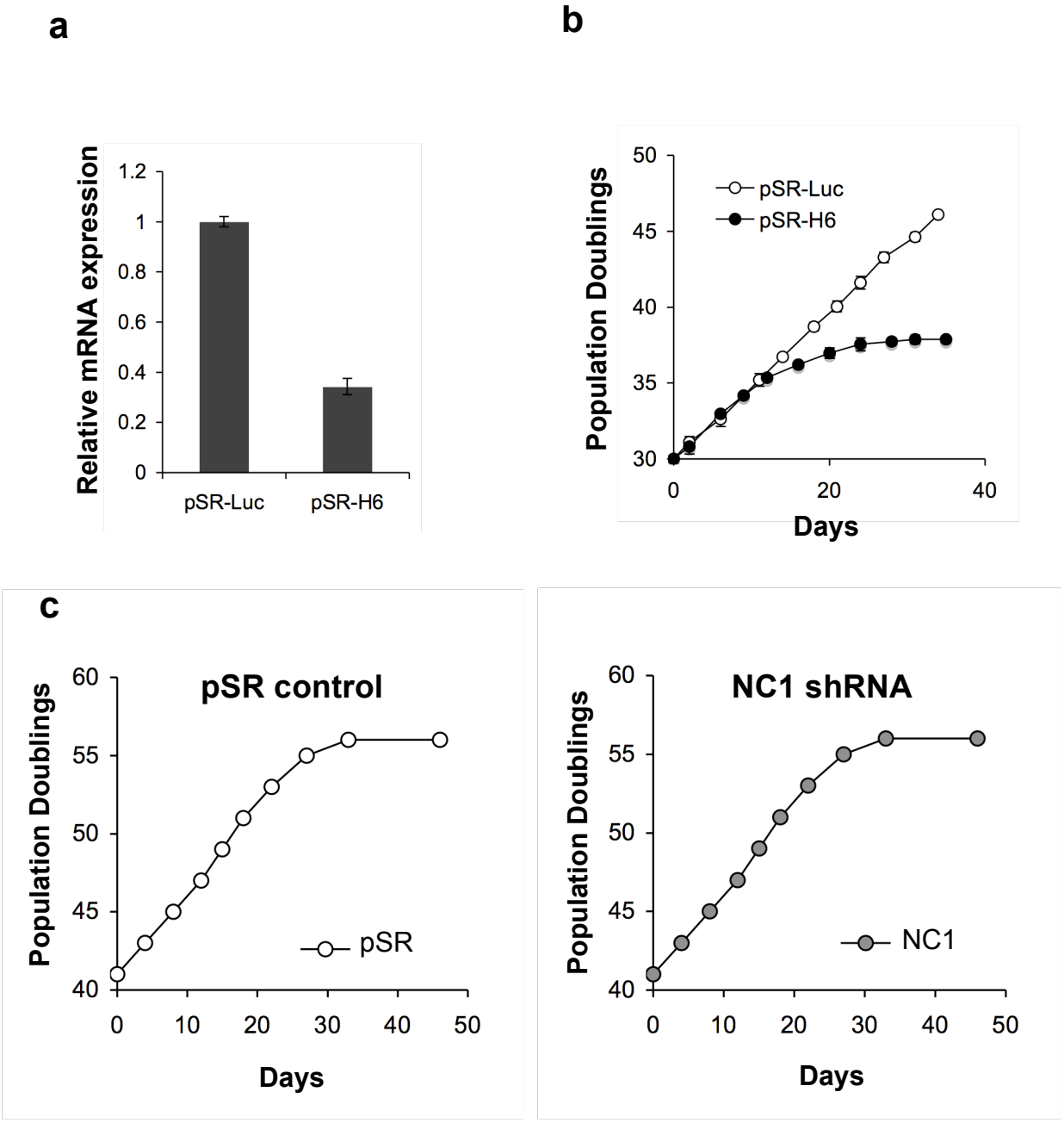

Supplemental Figure 3. Serial passaging experiments showing replicative histories of positive and negative control cells for comparison with SIRT6 knock-down cells in Figure 1b. **a**, Apollo expression levels in control (pSR-Luc) and Apollo knock-down (pSR-H6) WI-38 cells shown in (b), determined by qRT-PCR. **b,** Premature cellular senescence of WI-38 cells expressing an shRNA specific for the telomere accessory factor Apollo (pSR-H6). Note that the cells were infected at earlier PDs than in panels c and d, and in Figure 1b. **c, d**, Comparable replicative lifespans of WI-38 cells stably transduced with (right) an irrelevant shRNAs (NC1), or (left) control empty virus. NC1 shRNA Target sequence: CTTGTACGACGAAGACGAC. Similar results were obtained with two additional irrelevant shRNAs (data not shown).

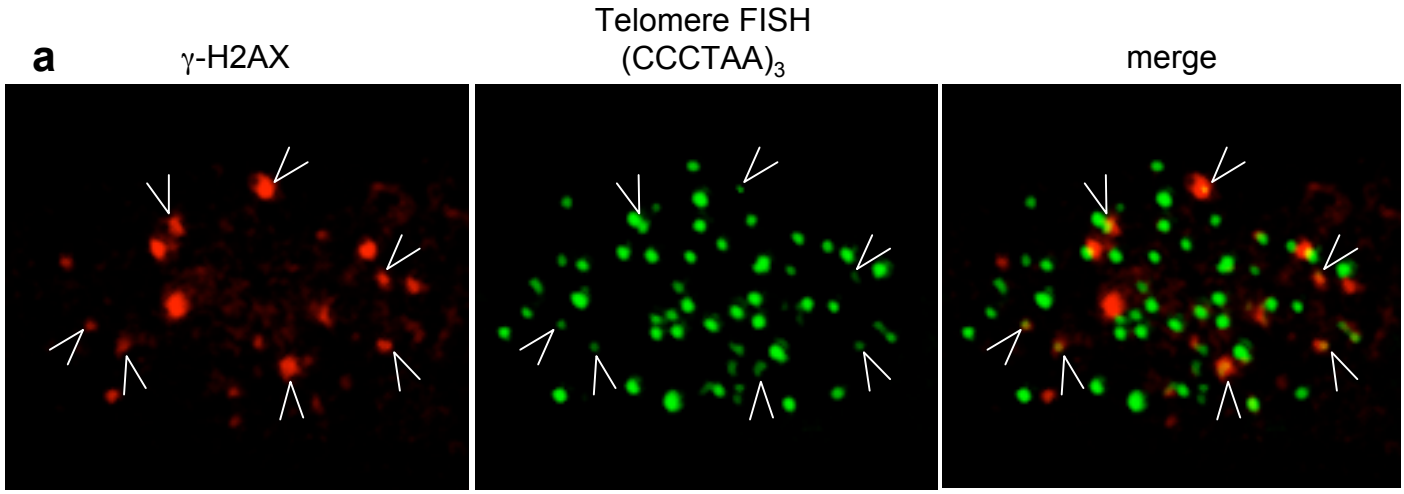

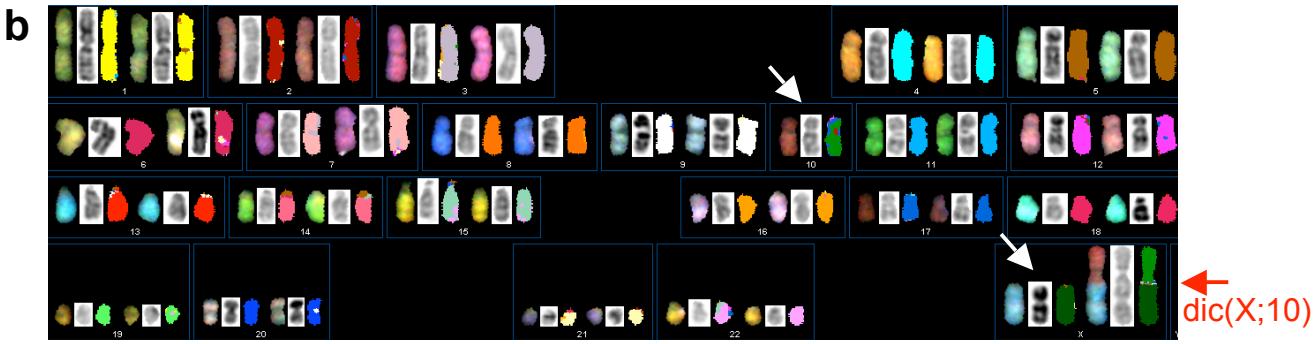

c

Experiment	Sample	PDs	Fusions (%)
WI-38 SKY	pSR	54	0
	S6KD	49	40
WI-38 T-FISH	pSR	54	0
	S6KD	49	27
IMR90 T-FISH	pSR	44	0
	S6KD	41	20
IMR90 DAPI	pSR	50	8
	S6KD	46	35

Supplemental Figure 4. Evidence for telomere dysfunction in SIRT6 knock-down cell. **a,** enlargement of images shown in Figure 1d. **b,** Spectral Karyotype (SKY) analysis of a representative S6KD metaphase showing a chromosomal end-to-end fusion between chromosomes X and 10 (dic(X;10)(pter;pter), red arrow). White arrows point to the other, normal X and 10 chromosomes. **c,** Increased chromosome end-to-end fusions in S6KD cells (generated with two independent shRNAs: $S6KD_1$ and $S6KD_2$) observed by several independent cytogenetic analyses. The cell type (IMR90 or WI-38) and cytogenetic method (SKY, DAPI, or Telomere FISH (T-FISH)) are indicated. Values represent the numbers of fused chromosomes observed as a percentage of total metaphases analyzed.

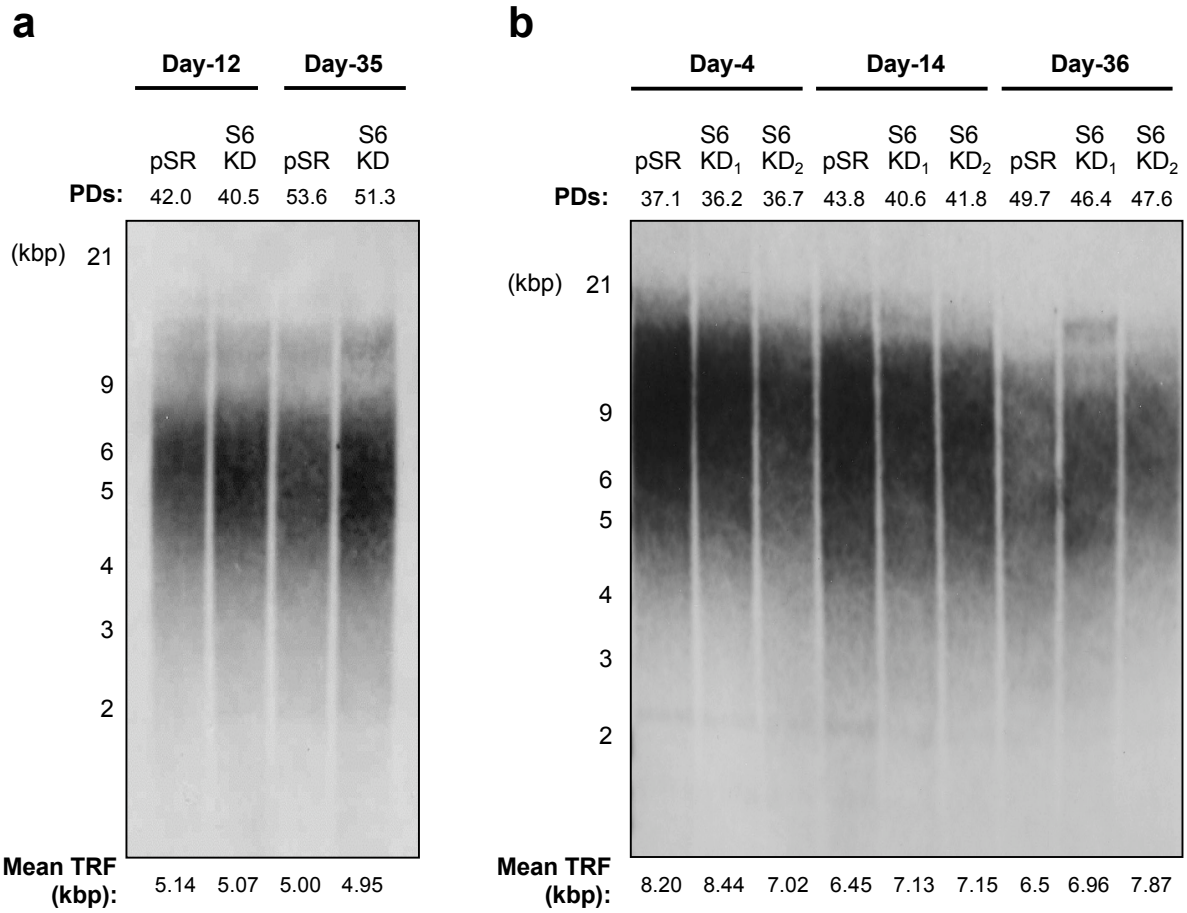

Supplemental Figure 5. Telomere Restriction Fragment (TRF) analysis of mean telomere length in S6KD and control pSR cells. **a**, WI-38 cells. **b**, IMR90 cells. The mean TRF lengths were determined as described by Harley C.B, et al (1). Samples were analyzed on the indicated days of serial passaging, and PD indicates the population doublings undergone in each sample.

(1) Harley, C.B. et al. (1990): Telomeres shorten during aging of human fibroblasts. Nature 345, 458-460.

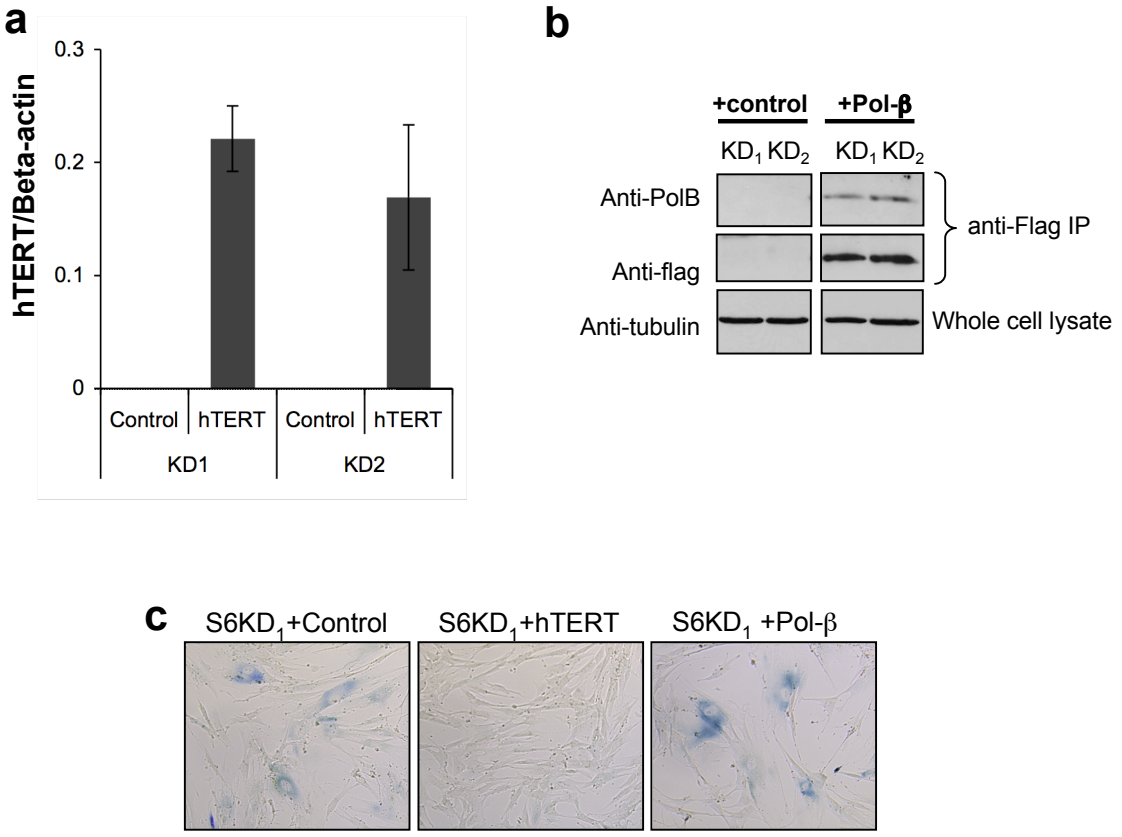

Supplemental Figure 6. Stabilizing telomeres via hTERT expression reverses the premature senescence of S6KD cells, whereas augmenting BER activity via expression of the Polb-dRP lyase domain does not rescue the S6KD defect. **a, b,** Expression of hTERT or Pol**β** (DNA polymerase beta dRP lyase domain) in the S6KD cells for functional complementation experiments shown in Figure 1g. **a,** Expression levels of hTERT detected by Taqman qRT-PCR analysis. Values are normalized to beta-actin levels. **b,** Expression of the Pol**β** dRP lyase domain, detected by Western analysis of Flag-tagged Pol**β**-dRP-lyase immunoprecipitated from WI-38 cells. **c,** Representative SA-β-gal staining for assay shown in Fig. 1g. The hTERT, Pol-β, or control empty vector were ectopically expressed in S6KD WI-38 cells, and passaged in physiologic (2%) oxygen conditions. Cells were stained with SA-β-gal at PD 36.5, to compare levels of senescent cells.

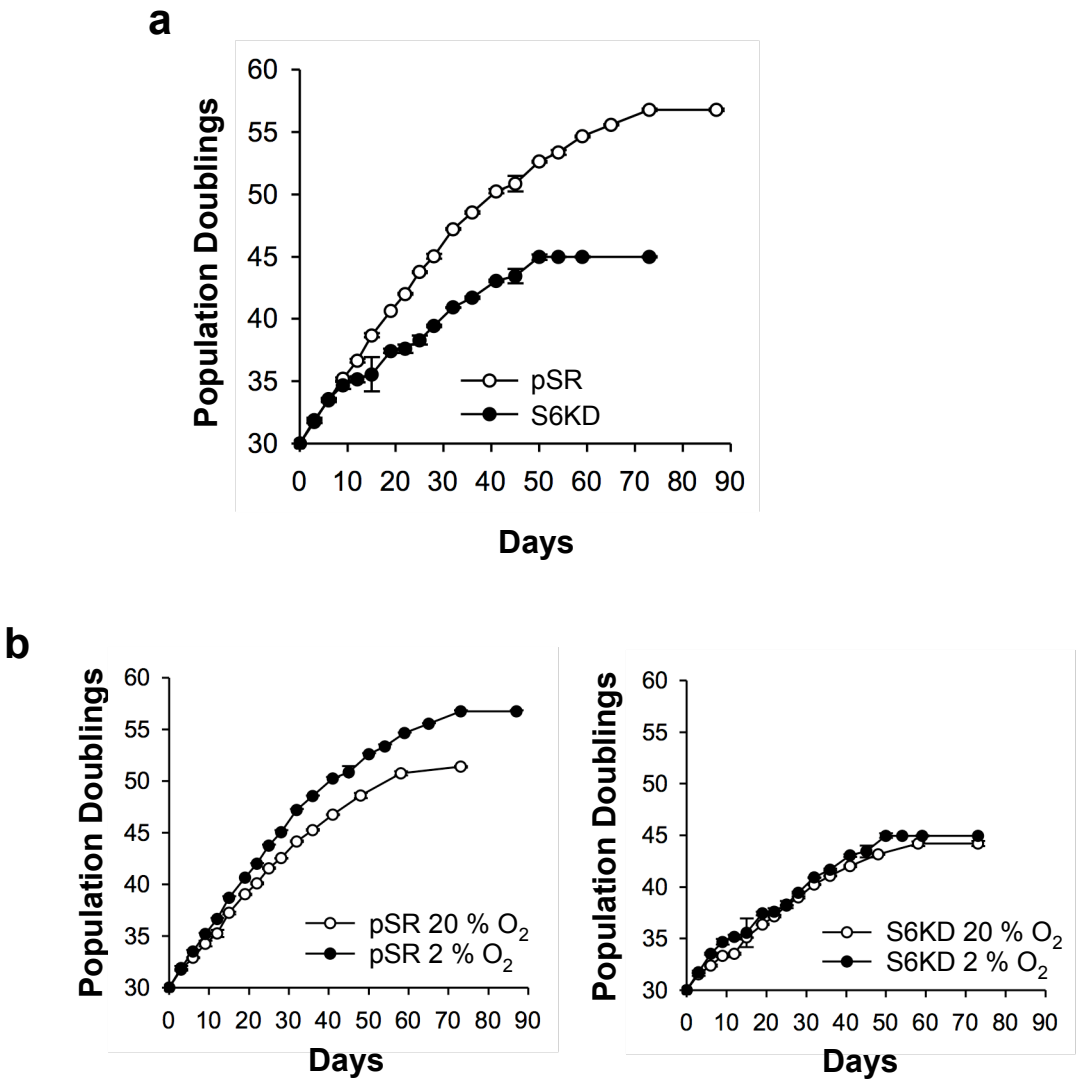

Supplemental Figure 7. Oxidative stress does not contribute to premature cellular senescence of SIRT6 knock-down (S6KD) WI-38 cells relative to control (pSR) cells. **a,** S6KD cells undergo premature cellular senescence when cultured under physiologic (2%) oxygen conditions. **b,** Lowering oxygen tension from 20% to 2% extends the replicative lifespan of SIRT6-proficient pSR cells (left), but has no significant effect on the replicative lifespan of S6KD cells (right).

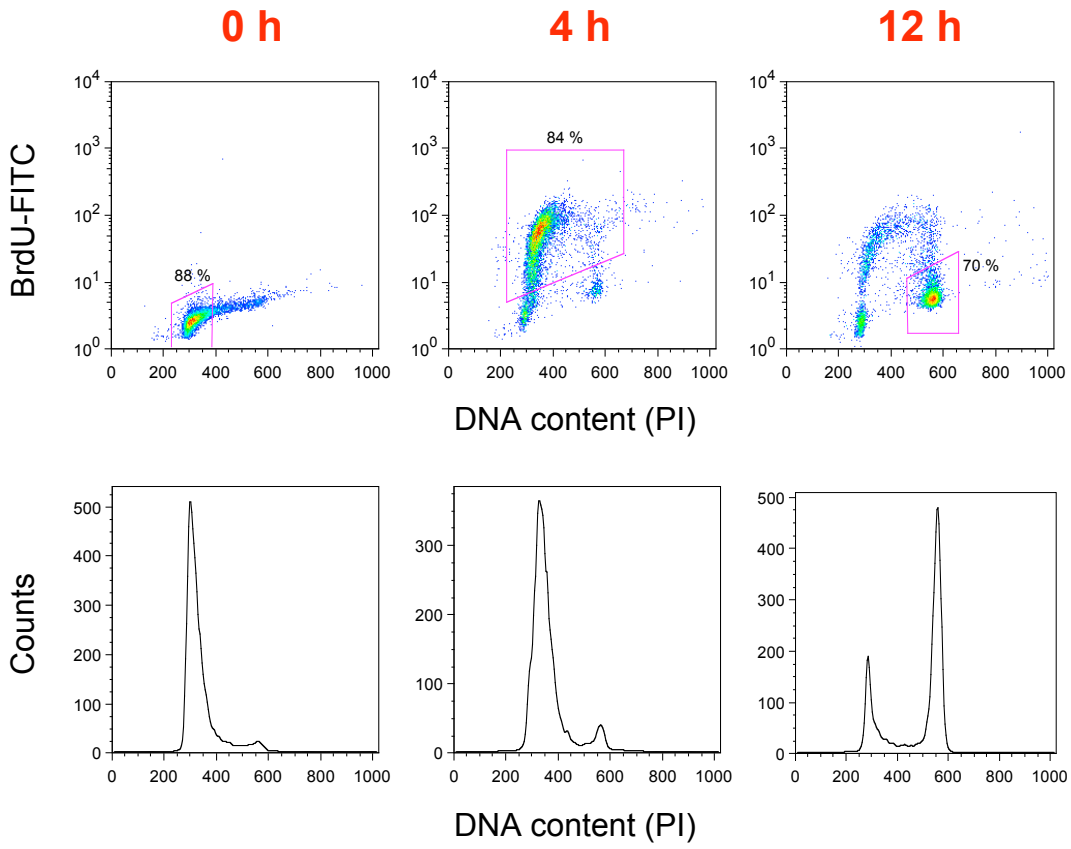

Supplemental Figure 8. Representative Flow Cytometry analysis of U2OS cells synchronized by a single thymidine block and released for the indicated times. Enrichment for G1, S, and G2/M phase cells is shown for 0, 4, and 12 hours, respectively. The data are plotted as both BrdU-PI profiles (top) and PI histograms (bottom).

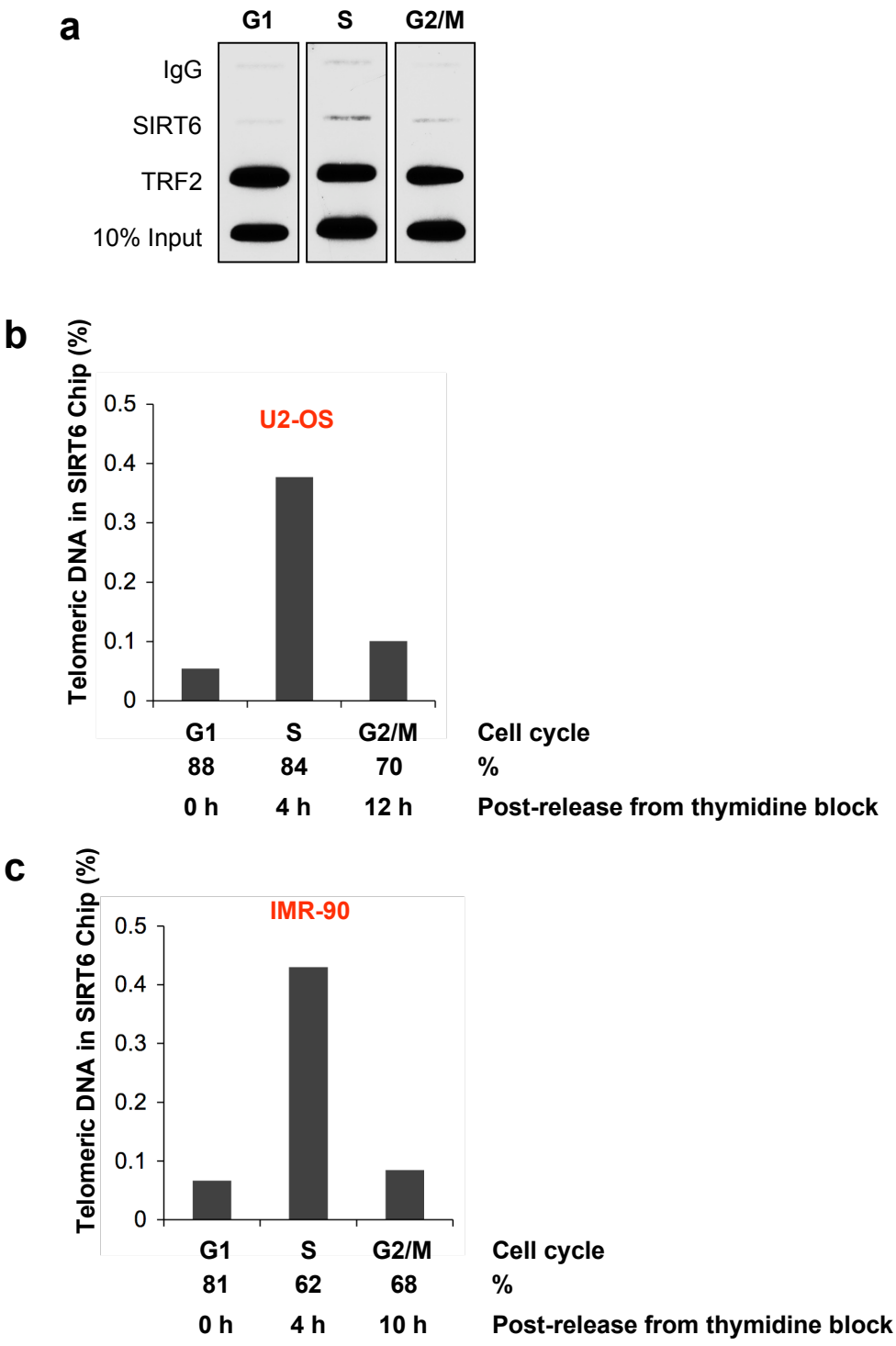

Supplemental Figure 9. SIRT6 associates specifically with telomeric chromatin in S-phase. **a,** Representative telomere ChIP analysis showing telomere sequences in SIRT6 ChIPs in S-phase enriched cultures, but not G1 or G2/M enriched cultures. IgG, negative control and TRF2 positive control ChIPs are shown for comparison. **b, c,** Quantitation of Telomere ChIP assays as shown in (a), conducted in U2OS **(b)** and IMR90 **(c)** cells. The percent of cells in the G1, S, and G2/M enriched cultures are indicated below the resepctive cell cycle phases.

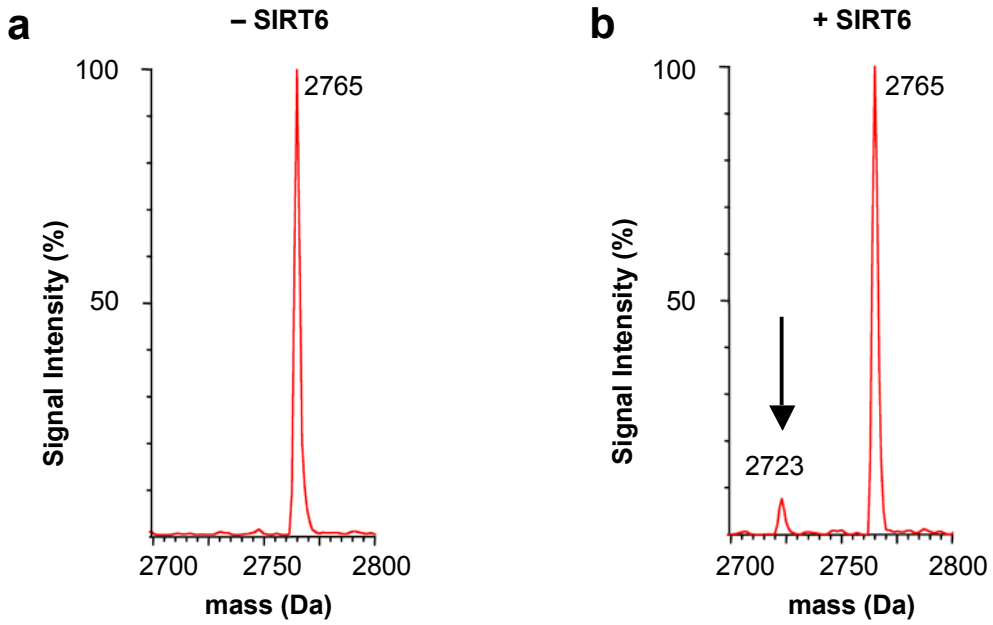

Supplemental Figure 10. Mass spectrometry analysis showing *in vitro* deactylation of an H3K9Ac peptide by recombinant SIRT6 protein (**a).** Arrow indicates the 2,723 Da peak corresponding to the deacetylated peptide. The acetylated peptide in a control reaction without SIRT6 is shown for comparison (**b)**.

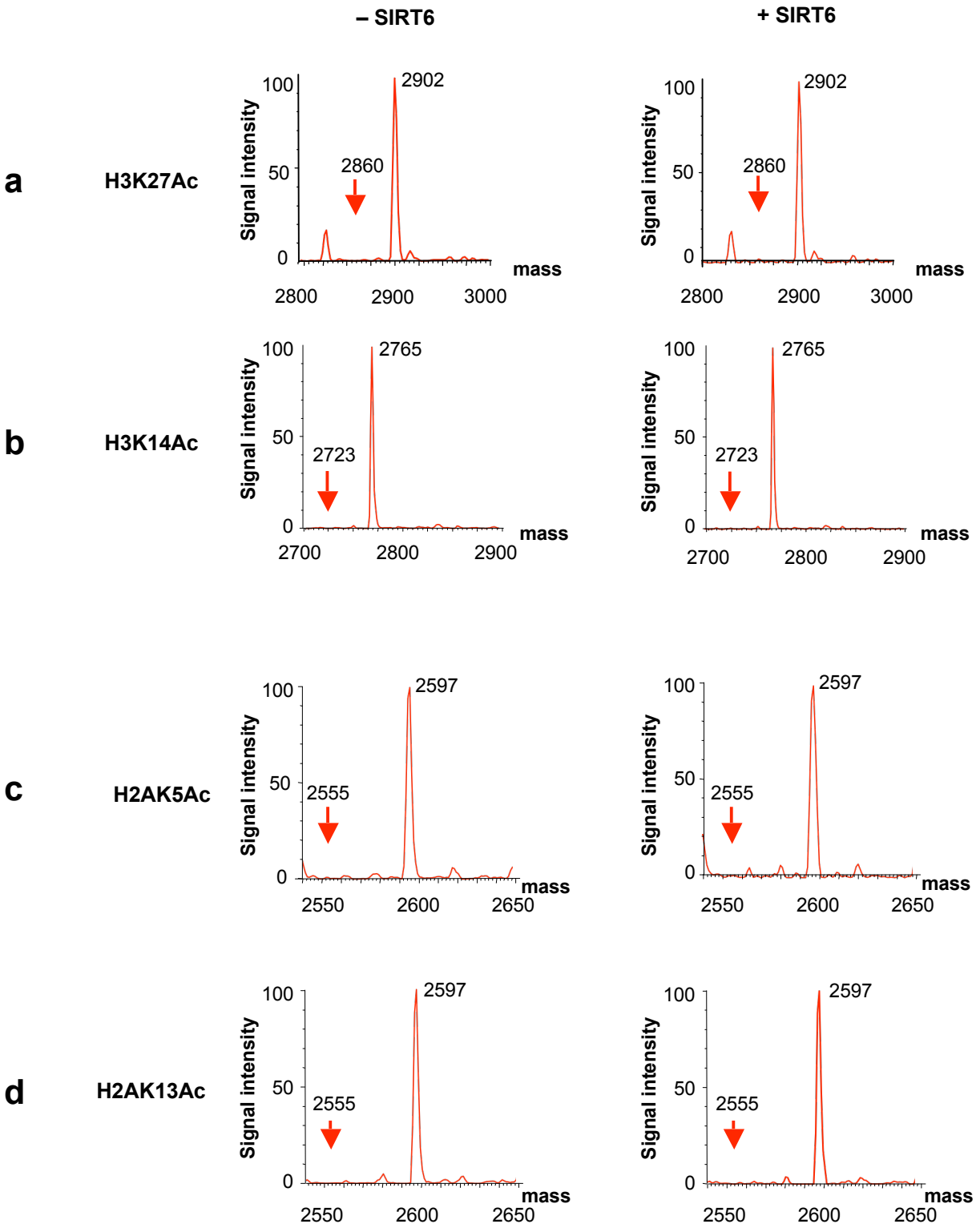

Supplemental Figure 11. SIRT6 does not deacetylate numerous acetylated histone peptides. Arrows indicated predicted size of the unacetylated peptide.

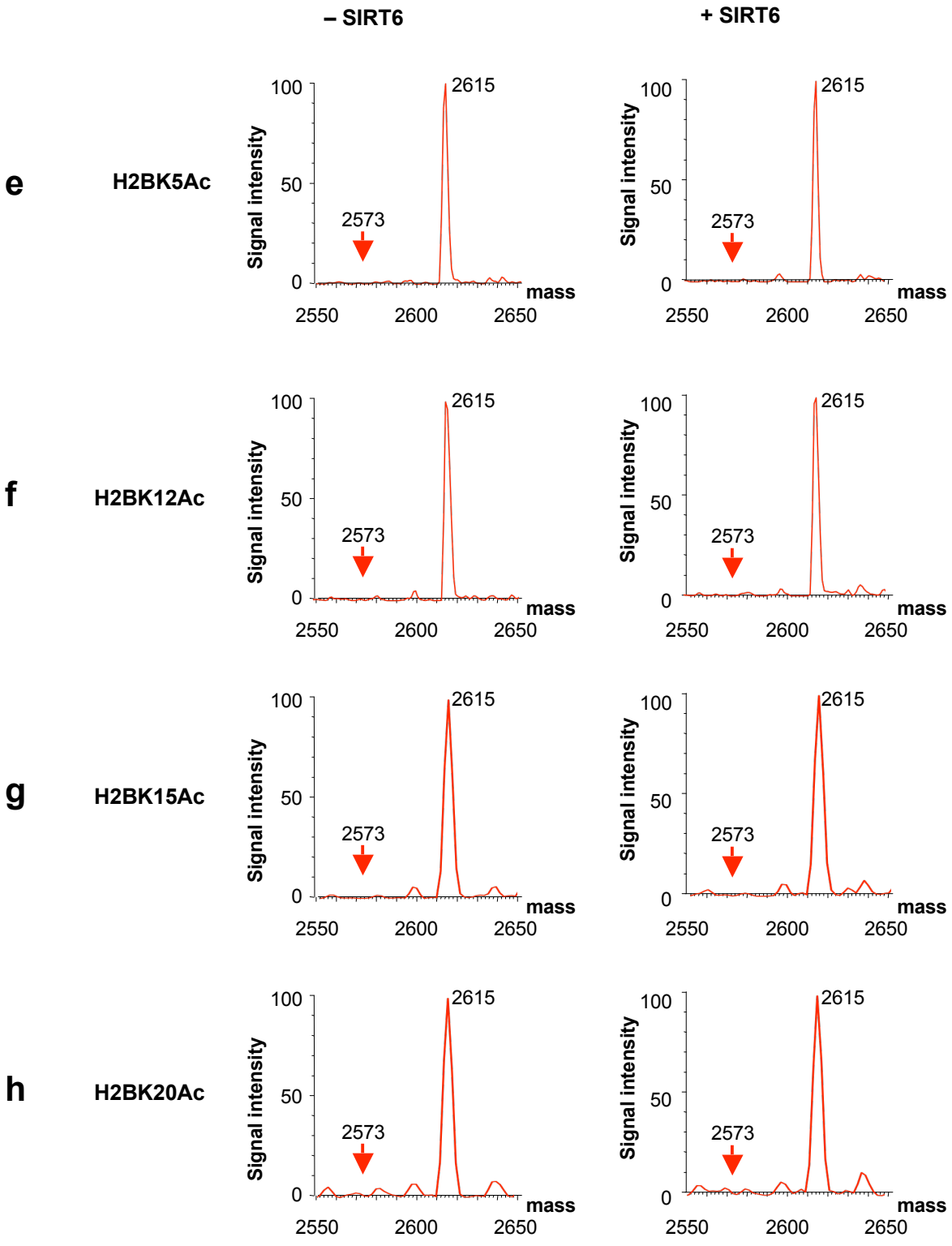

Supplemental Figure 11. SIRT6 does not deacetylate numerous acetylated histone peptides. Arrows indicated predicted size of the unacetylated peptide.

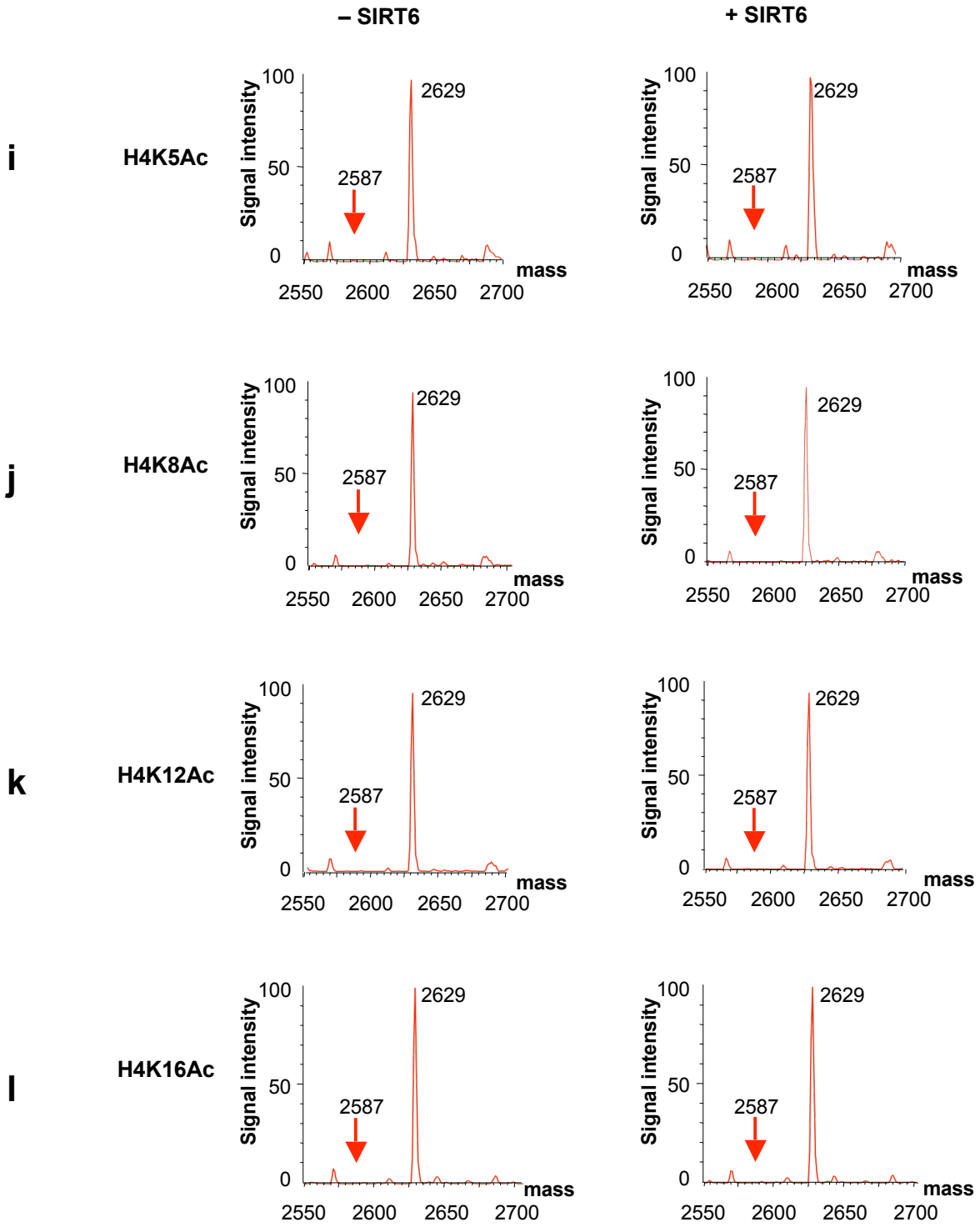

Supplemental Figure 11. SIRT6 does not deacetylate numerous acetylated histone peptides. Arrows indicated predicted size of the unacetylated peptide.

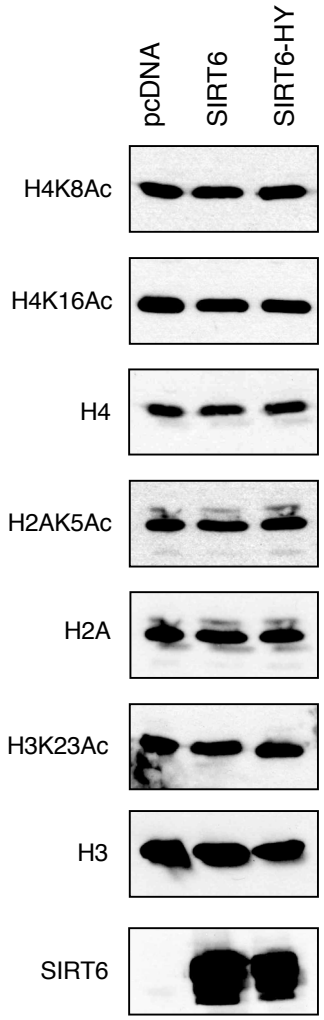

Supplemental Figure 12. SIRT6 does not deacetylate numerous acetylated histone tail residues. Western analysis of whole cell lysates following over-expression of wild-type SIRT6, catalytic mutant SIRT6-HY, or pcDNA empty vector, with the indicated antibodies.

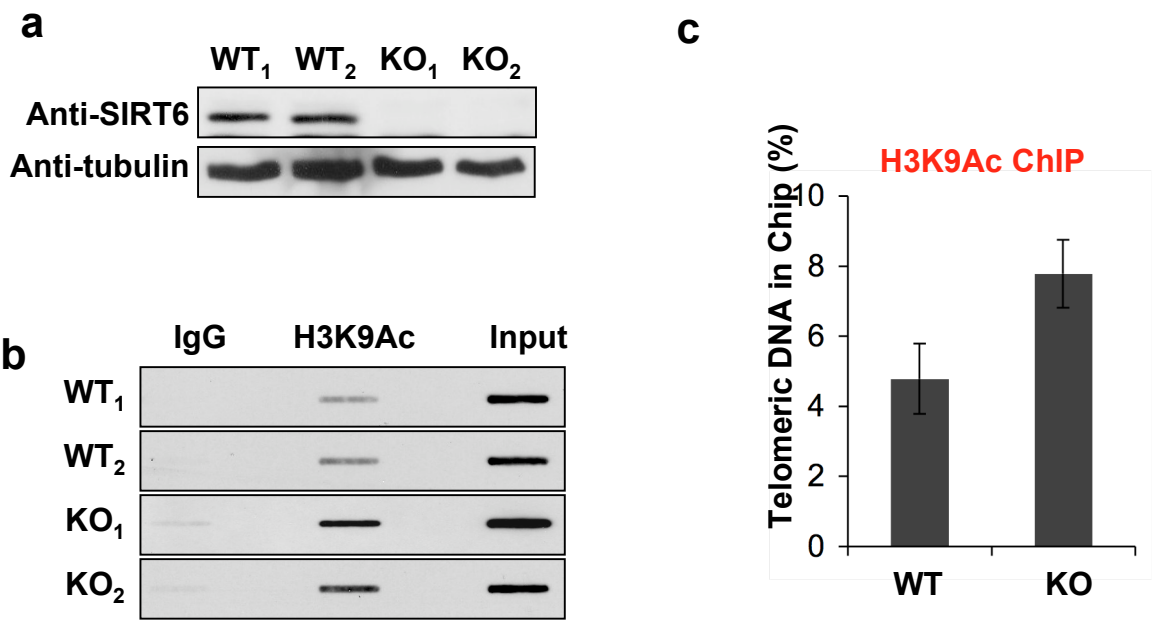

d

Telomere FISH Analysis of Chromosome fusions

	Fusions	Chromosomes
WT	0	477
KO	0	711

e

SIRT6 T-FISH in WRN-deficient cells

	Telomeric DNA in Chip (%)
AG11395	0.33%
U2OS	0.38% 0.30% 0.53%

Supplemental Figure 13. Telomeric histone H3K9 hyperacetylation without telomere functional aberrations in SIRT6 knockout (S6KO) mouse cells. **a,** SIRT6 expression in S6KO mouse embryonic fibroblasts (MEFs) and WT littermate controls. Generation of the S6KO mice by Regeneron Pharmaceuticals and Western analysis of S6 protein were as previously described (1). **b, c,** H3K9 is hyperacetylated at telomeric chromatin in S6KO MEFs. Telomere ChIP analysis with anti-H3K9Ac antibodies. **d,** No increased chromosome end-to-end fusions observed in S6KO MEFs. Summary of telomere FISH analysis of metaphase spreads prepared from S6KO and wild-type littermate control cells. **e,** Association of SIRT6 with telomeric chromatin in WRN-deficient cells (AG11395, Werner Syndrome patient cell line). Data from WRN-proficient U2OS cells are shown for comparison.

(1) Mostoslavsky, R. et al. (2006): Genomic instability and aging-like phenotype in the absence of mammalian SIRT6. Cell *124*, 315-329.

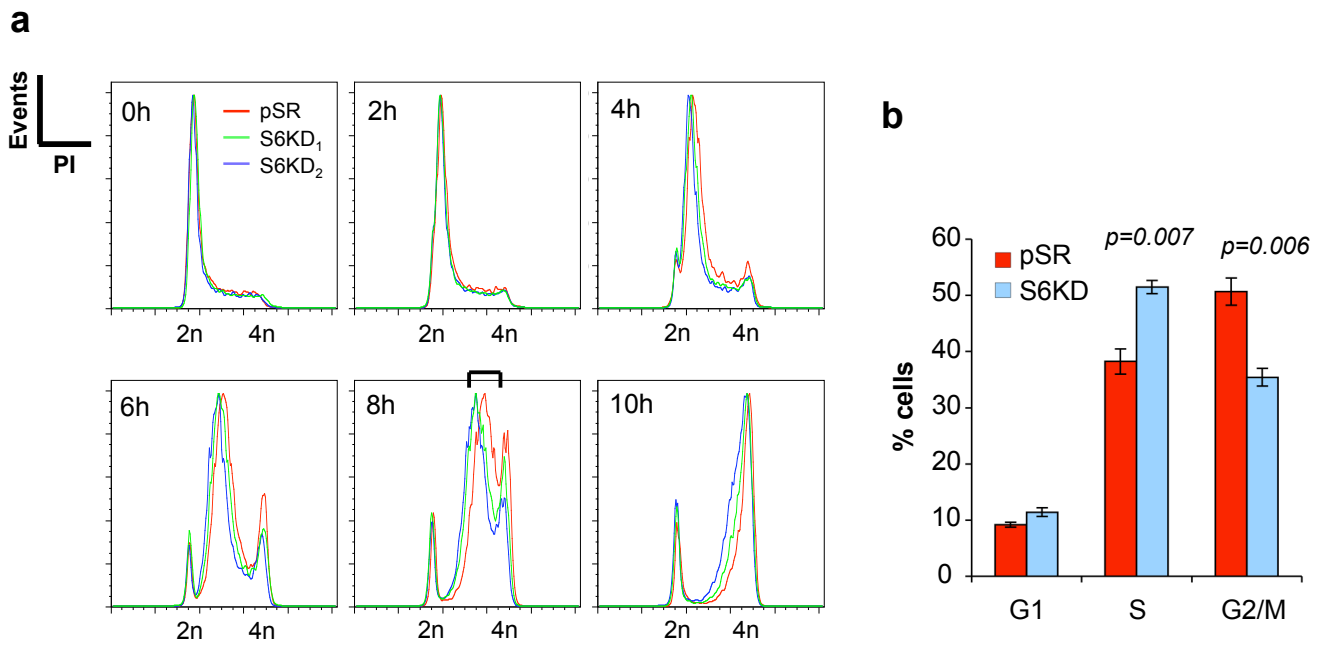

Supplemental Figure 14. g, Flow cytometry analysis showing delayed S-phase completion in S6KD U2OS cells. Representative cell cycle profiles of $S6KD_1$ (green), $S6KD_2$ (blue), and control pSR (red) U2OS cells, at the indicated time-points after release from a thymidine block. DNA content (2n and 4n) determined by of Propidium Iodide (PI) staining is indicated. Bracket highlights delay in S-phase completion in the S6KD cells at 8h, when it is most clear. **b,** Quantitation of cell cycle profiles showing S-phase delay in S6KD U2OS cells as shown in (a).